Atherosclerosis 288 (2019) 175–185

Contents lists available at ScienceDirect

Atherosclerosis

journal homepage: www.elsevier.com/locate/atherosclerosis

Correlation of computed tomography with carotid plaque transcriptomes associates calcification with lesion-stabilization

Eva Karlöf[a,b], Till Seime[b], Nuno Dias[c], Mariette Lengquist[b], Anna Witasp[d], Håkan Almqvist[e], Malin Kronqvist[b], Jesper R. Gådin[f], Jacob Odeberg[g], Lars Maegdefessel[f,h], Peter Stenvinkel[d], Ljubica Perisic Matic[b,**,1], Ulf Hedin[a,b,*,1]

[a] Department of Vascular Surgery, Karolinska University Hospital, Stockholm, Sweden
[b] Department of Molecular Medicine and Surgery, Karolinska Institutet, Stockholm, Sweden
[c] Vascular Center, Department of Vascular Surgery, Skåne University Hospital, Malmö, Sweden
[d] Division of Renal Medicine, Department of Clinical Sciences, Intervention and Technology, Karolinska Institutet, Stockholm, Sweden
[e] Department of Clinical Neuroscience, Karolinska Institutet, Stockholm, Sweden
[f] Department of Medicine, Center for Molecular Medicine, Karolinska Institutet, Stockholm, Sweden
[g] Science for Life Laboratory, Department of Proteomics, School of Biotechnology, Royal Institute of Technology, Stockholm, Sweden
[h] Department of Vascular and Endovascular Surgery, Klinikum Klinikum rechts der Isar Isar, Technical University Munich, Munich, Germany

HIGHLIGHTS

- Macro-calcification in carotid lesions was assessed by CTA and microarrays.
- Calcification was linked to a transcriptional profile typical for stable plaques.
- PRG4 was enriched in calcified ECM and localized to activated macrophages and SMCs.
- Assessment of calcification may aid evaluation of plaque phenotype and stroke risk.

ARTICLE INFO

Keywords:
Atherosclerosis
Computed tomography
Microarrays
Calcification
Carotid stenosis
Smooth muscle cells

ABSTRACT

Background and aims: Unstable carotid atherosclerosis causes stroke, but methods to identify patients and lesions at risk are lacking. We recently found enrichment of genes associated with calcification in carotid plaques from asymptomatic patients. Here, we hypothesized that calcification represents a stabilising feature of plaques and investigated how macro-calcification, as estimated by computed tomography (CT), correlates with gene expression profiles in lesions.
Methods: Plaque calcification was measured in pre-operative CT angiographies. Plaques were sorted into high- and low-calcified, profiled with microarrays, followed by bioinformatic analyses. Immunohistochemistry and qPCR were performed to evaluate the findings in plaques and arteries with medial calcification from chronic kidney disease patients.
Results: Smooth muscle cell (SMC) markers were upregulated in high-calcified plaques and calcified plaques from symptomatic patients, whereas macrophage markers were downregulated. The most enriched processes in high-calcified plaques were related to SMCs and extracellular matrix (ECM) organization, while inflammation, lipid transport and chemokine signaling were repressed. These findings were confirmed in arteries with high medial calcification. Proteoglycan 4 (*PRG4*) was identified as the most upregulated gene in association with plaque calcification and found in the ECM, SMA+ and CD68+/TRAP + cells.
Conclusions: Macro-calcification in carotid lesions correlated with a transcriptional profile typical for stable plaques, with altered SMC phenotype and ECM composition and repressed inflammation. PRG4, previously not described in atherosclerosis, was enriched in the calcified ECM and localized to activated macrophages and smooth muscle-like cells. This study strengthens the notion that assessment of calcification may aid evaluation of plaque phenotype and stroke risk.

* Corresponding author. Department of Molecular Medicine and Surgery L8:03, Karolinska Institutet, SE-171 76, Stockholm, Sweden.
** Corresponding author.
E-mail addresses: Ljubica.Matic@ki.se (L.P. Matic), Ulf.Hedin@ki.se (U. Hedin).
[1] These authors contributed equally to this work.

https://doi.org/10.1016/j.atherosclerosis.2019.05.005
Received 3 September 2018; Received in revised form 29 April 2019; Accepted 8 May 2019
Available online 11 May 2019

1. Introduction

Unstable atherosclerosis in the carotid bifurcation has been linked to approximately 10–20% of all ischemic strokes [1]. It is difficult to estimate precisely to what extent carotid plaques contribute to extracranial atheroembolism as we lack imaging modalities capable of identifying unstable lesions [2]. Today, risk assessment based on the degree of luminal narrowing by stenosis yields moderate procedural efficacy for stroke-preventive surgery (carotid endarterectomy, CEA) in symptomatic patients and questionable efficacy for asymptomatic ones [3]. New imaging modalities are therefore being developed to identify high-risk lesions and improve stroke prevention. Understanding the biological processes that underlie morphological plaque features recognized by these modalities would strengthen their predictive power in selection of patients for intervention [2].

Unstable atherosclerotic plaques are characterized by disruption of the protective fibrous cap, endothelial erosions, enhanced inflammation, large lipid-rich necrotic cores and intraplaque haemorrhage, while stable lesions typically contain more smooth muscle cells (SMCs) and fibrous tissue [4]. In atherogenesis, contractile SMCs modulate into a proliferative and synthetic phenotype that migrates from the media into the intima, secrete extracellular matrix (ECM) components and build the fibrous cap [5]. Within lesion, SMCs have been assigned broad phenotypic plasticity [5–7] and reported to coexist in various intermediate phenotypes. In a recent study, we have shown that SMCs in carotid atherosclerosis downregulate classical and hitherto unknown markers for cytoskeletal integrity as well as calcium (Ca) signaling (i.e. *ACTA2, MYH11, PDLIM7, SYNPO2, LMOD1, PLN*) [8].

Calcification is a prominent feature of end-stage atherosclerosis, but it is also typical for the artery media of patients with chronic kidney disease (CKD) [9,10]. Vascular calcification can be influenced by altered Ca and phosphate homeostasis, loss of mineralization inhibitors and dysfunction of natural regulators in bone metabolism such as osteopontin, osteoprotegerin, matrix-gla protein, fetuin-A and receptor activator of NF-κB. Whereas intimal calcification is coupled to plaque inflammation and lipid deposition, medial calcification involves toxic metabolite-induced vascular changes that promote osteogenic differentiation and subsequent matrix mineralization. Clinically, medial calcification leads to arterial stiffness and increased pulse pressure, while the consequences of intimal calcification are less clear [11]. Moreover, intimal micro- and macro-calcification have been suggested to influence plaque stability differently [12,13], however, the impact of size, composition, and distribution of calcification in plaque vulnerability, remains unclear. Computerized tomography (CT) images calcifications in atherosclerosis [13] and scoring of coronary artery calcification by CT (CAC score) has been implemented in prediction of cardiovascular risk. High CAC score confers increased cardiovascular risk [13], whereas carotid plaque calcifications seem to be associated with reduced stroke risk [14,15].

We and others [16,17] recently confirmed that molecular pathways related to calcification dominate in end-stage carotid plaques. While osteolytic processes, suggesting reduced calcification, were prevalent in plaques from symptomatic patients, plaques from patients on statin therapy and asymptomatic ones were enriched in processes associated with increased calcification [8]. To investigate this further, here we focused on the transcriptome of calcified carotid plaques, by selecting patients with different degrees of calcification as estimated by preoperative CT angiographies (CTA) and analysed global gene expression profiles in corresponding CEA specimens using microarrays. We show that high-calcified lesions were enriched in molecular processes associated with SMC function, ECM organization and calcification, while inflammation, lipid metabolism and chemokine signaling were repressed.

2. Materials and methods

2.1. Human carotid atherosclerosis cohort

Patients undergoing surgery for high-grade (> 50% NASCET) [18] carotid stenosis at the Department of Vascular Surgery, Karolinska University Hospital, Stockholm, Sweden were consecutively enrolled in the study and clinical data recorded on admission. Patients with high vs. low calcified carotid lesions on CTA were selected for the study. Symptoms (S) were defined as transitory ischemic attack (TIA), minor stroke (MS) and *amaurosis fugax* (retinal TIA). Patients without qualifying symptoms within 3 months prior to surgery were categorised as asymptomatic (AS) and indication for CEA based on results from the Asymptomatic Carotid Surgery Trial (ACST) [19]. Carotid endarterectomies (carotid plaques, CP) were collected at surgery and retained within the Biobank of Karolinska Endarterectomies (BiKE). The study cohort demographics, details of sample collection and processing and transcriptomic analyses by microarrays were as previously described in details [8,20,21] and shown in Supplementary Tables I and II Briefly, plaques were divided transversally at the most stenotic part; the proximal half of the lesion was used for RNA preparation while the distal half was immediately fixed in 4% formaldehyde for 48 h. Highly calcified specimens planned for histological analyses, were first decalcified in Modified Decalcification Solution (formic acid; Histolab, Gothenburg, Sweden) for 5 days, and all specimens were dehydrated in graded ethanol and embedded in paraffin.

All human samples were collected with informed consent from patients; studies were approved by the regional Ethical Committee and follow the guidelines of the Declaration of Helsinki.

2.2. Computed tomography angiography (CTA) examination and image analysis

Carotid CTA was performed as a pre-operative routine at the admitting hospital using site-specific image acquisition protocols (examination protocols in Supplementary Table III). CTA exams were performed between March 2008 and October 2013, in 7 different CT-labs at 5 hospitals, using 3 vendors and in total 4 different models. In summary, CTA exams were performed with 100 or 120 kVp, variation of CTDIvol16cm between 13.9 and 36.9 mGy or CTDIvol32cm 7.9–28.3 mGy. Contrast injection rate and amount followed by a saline chaser were at the discretion of the local hospitals. Briefly, a caudocranial scanning direction was selected from the aortic arch to the vertex, using intravenous contrast. An axial image reconstruction of 0.625 mm (in 37 exams; 0.9 mm in two exams; and 1 mm in one exam) was obtained and transferred into a digital workstation for vascular CT-scan image analysis using the Plaque Analysis application of the TeraRecon software (iNtuition, TeraRecon, Foster City, CA, USA). A centreline of flow was semi-automatically placed from the common to the internal carotid artery. The area of the atherosclerotic plaque was manually selected using the common carotid bifurcation as a reference point. The outer and inner borders of the artery wall were automatically defined, adjusted manually, the lumen was excluded from the analysis and artery wall volumes automatically calculated within 5 different levels of Hounsfield Units (HU) with standardised cut-offs (−150 HU to 0 HU; 1 HU to 129 HU; 130 HU to 199 HU; 200 HU to 299 HU; 300 HU to 399 and 400 HU to 3000 HU). The analysis provided a semi-automatically generated calcium volume of the carotid plaque, which was analysed with a threshold of 400 Hounsfield Units (HU) for calcification and a ratio was calculated (Vcalc/Vtot = calcification degree). The measurements of CT images were done by the same observer (E. K.) and blinded to histological and biochemical analysis. The measurements were restricted to the most proximal half of the plaque with cutoff level

at tightest stenosis, in order to correlate CTA to the corresponding plaque microarray analysis.

2.3. Bioinformatic and statistical analyses

Transcriptomic dataset was pre-processed using Bioconductor software. For the initial discovery, group analyses were performed by a two-sided Student's t-test assuming non-equal deviation with correction for multiple comparisons according to Bonferroni, as previously described [8,21]. Subsequently, to confirm the most important results presented in the study, a linear regression model was used with calcification as the continuous variable. Graphs were generated using GraphPad Prism 6. Discovery analyses of highly significantly dysregulated genes were performed by comparing patients with the 10 most highly calcified plaques (30–65%) *vs.* 10 least calcified ones (0–2%), as well as 7 symptomatic *vs.* 7 asymptomatic patients from the high-calcified group, while the whole cohort of 40 patients was used for validation of results. Following differential gene expression, gene set enrichment analyses on Gene Ontology (GO) terms were performed using several public softwares for comparison: GeneMania (www.genemania.org), GOrilla (http://cbl-gorilla.cs.technion.ac.il) and ENRICHR (http://amp.pharm.mssm.edu/Enrichr). Final data presented was from GOrilla including filtering of overlapping GO categories was performed using Revigo software (http://revigo.irb.hr). Functional data about the genes was extracted using GeneCards (www.genecards.org) and PubMed literature search. Pearson correlations were calculated to determine the association between mRNA expression levels from microarrays. Large-scale overall correlation analyses were conducted using Morpheus software (http://software.broadinstitute.org/morpheus). The minimal gene signature/combined panel predicted for separating two groups of patients was analysed using the default settings of the 'Marker prediction' tool in the Morpheus software, Broad Institute and based on the whole microarray dataset, taking into account differential gene expression and 100 permutations for obtaining the prediction accuracy. Principal components (PCA) analysis was performed using ClustVis software (https://biit.cs.ut.ee/clustvis_large/). To enumerate the relative abundance of cellular populations in the tissue composition, we applied the mRNA deconvolution strategy to microarrays using the Cibersort web software (https://cibersort.stanford.edu). In this analysis, immune cell populations were deconvoluted using a publicly available expression file containing signature markers for 22 different leukocyte subtypes [22]. Cell compartments localization data was analysed using the SubCellBarCode software (http://subcellbarcode.org) [23] and based on the differentially expressed genes between high vs. low calcified plaques. In all analyses adjusted $p < 0.05$ was considered to indicate statistical significance.

Additional Material and Methods are described in Supplementary Data.

3. Results

3.1. Study design and CTA classification of plaque calcification

Patients undergoing CEA (n = 40 totally) were enrolled in the study by: i) assesment of the calcification grade in pre-operative CTA, ii) matching concerning symptomatology, comorbidities, age, gender, and iii) quality of RNA material extracted from plaques (Fig. 1A). Overall, plaques were categorised into high-calcified (18–65% calcification;

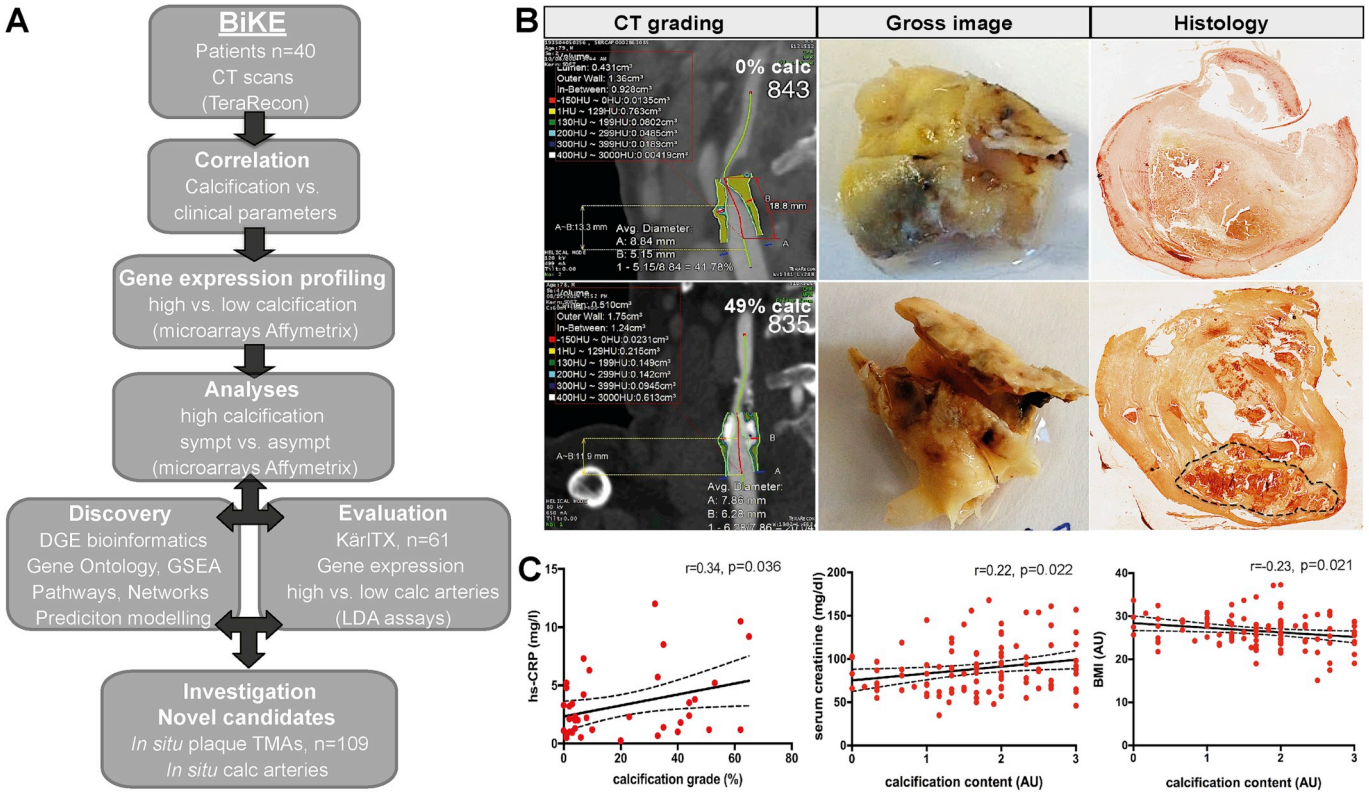

Fig. 1. Study workflow.
(A) Carotid plaques (n = 40 patients) were classified into high- and low-calcified by pre-operative CTA and profiled by microarrays, followed with bioinformatic analyses. Results were evaluated in an independent cohort of arteries (n = 61) with medial calcification and by large-scale *in situ* technologies (tissue microarrays, n = 109). (B) Representative CTA images of high- and low-calcified plaques, gross morphology and histology of calcification (dotted line) by Alizarin Red staining. (C) Plaque calcification estimated by CTA or Alizarin red content positively associates with hsCRP and creatinine levels, but negatively with BMI. *$p < 0.05$, **$p < 0.01$, ***$p < 0.001$, ****$p < 0.0001$. (For interpretation of the references to color in this figure legend, the reader is referred to the Web version of this article.)

n = 18 patients) and low-calcified (0–10%; n = 22; Fig. 1B), and global gene expression in plaques was profiled by microarrays followed by bioinformatic analyses. To increase significance for discovery of dysregulated genes in calcification, analyses were initially performed in two well-separated groups of the 10 most calcified plaques (30–65%) *vs.* the 10 least calcified ones (0–2%), while the whole cohort was used in validation. In order to investigate the molecular profile of calcification with respect to patient symptomatology, analyses were also made within the high-calcified group of plaques comparing those from symptomatic (n = 7) *vs.* asymptomatic (n = 7) patients. The most significant findings from these analyses were then investigated an independent cohort of arteries with medial calcification (n = 61, Supplementary Table II). In addition, plaque calcification was estimated histologically by Alizarin red staining of lesions and the most significant findings were semi-quantitated using tissue microarrays (TMAs; n = 109 patients).

There were no significant differences between high and low calcified patient groups with respect to general characteristics, symptomatology, smoking or medical treatment (Supplementary Table I). Correlation analysis between plaque calcification estimated by CTA or histology and clinical parameters (Supplementary Table IV), showed positive association only with plasma hs-CRP and creatinine, while association was negative with BMI (Fig. 1C).

3.2. Calcification associates with enrichment of smooth muscle related pathways and repression of inflammation

Global gene expression analysis comparing high vs. low calcified plaques resulted in 3387 significantly differentially expressed probesets, of which 1783 were upregulated and 1604 downregulated (of totally 70526 microarray probesets, Bonferroni adjusted $p < 0.05$, Supplementary Tables V and VI). There was a striking upregulation of typical SMC contractility markers such as *CNN1, ACTA2, MYOCD* (Fig. 2A) and even sensitive markers recently shown to be downregulated in carotid plaques in general (*SYNPO2, LMOD1, PDLIM7, MYH11, PLN,* all $p < 0.0001$, Supplementary Table V) [21]. This was accompanied by upregulation of ECM-related genes such as ELN, collagens, integrins and proteoglycans (i.e. *PRG4, CSPG4, HSPG2*). In contrast, markers of macrophages (*CD68, MARCO, CD36*), lipid turnover (*LPL, APOC1, PLIN2, ALOX5*), ECM degradation (*MMP7, MMP8, MMP9, MMP12*, cathepsins) and chemokines (*CCL18, CCL3, CCL4, CXCR4, IL8*, all $p < 0.0001$) were downregulated (Fig. 2B, Supplementary Table VI). The data was validated *in silico* by microarrays from the whole cohort of 40 patients comparing high *vs.* low calcified groups, and additionally using the linear regression model (Supplementary Fig. IA, Supplementary Table VII).

Gene set enrichment and pathway analyses on significantly

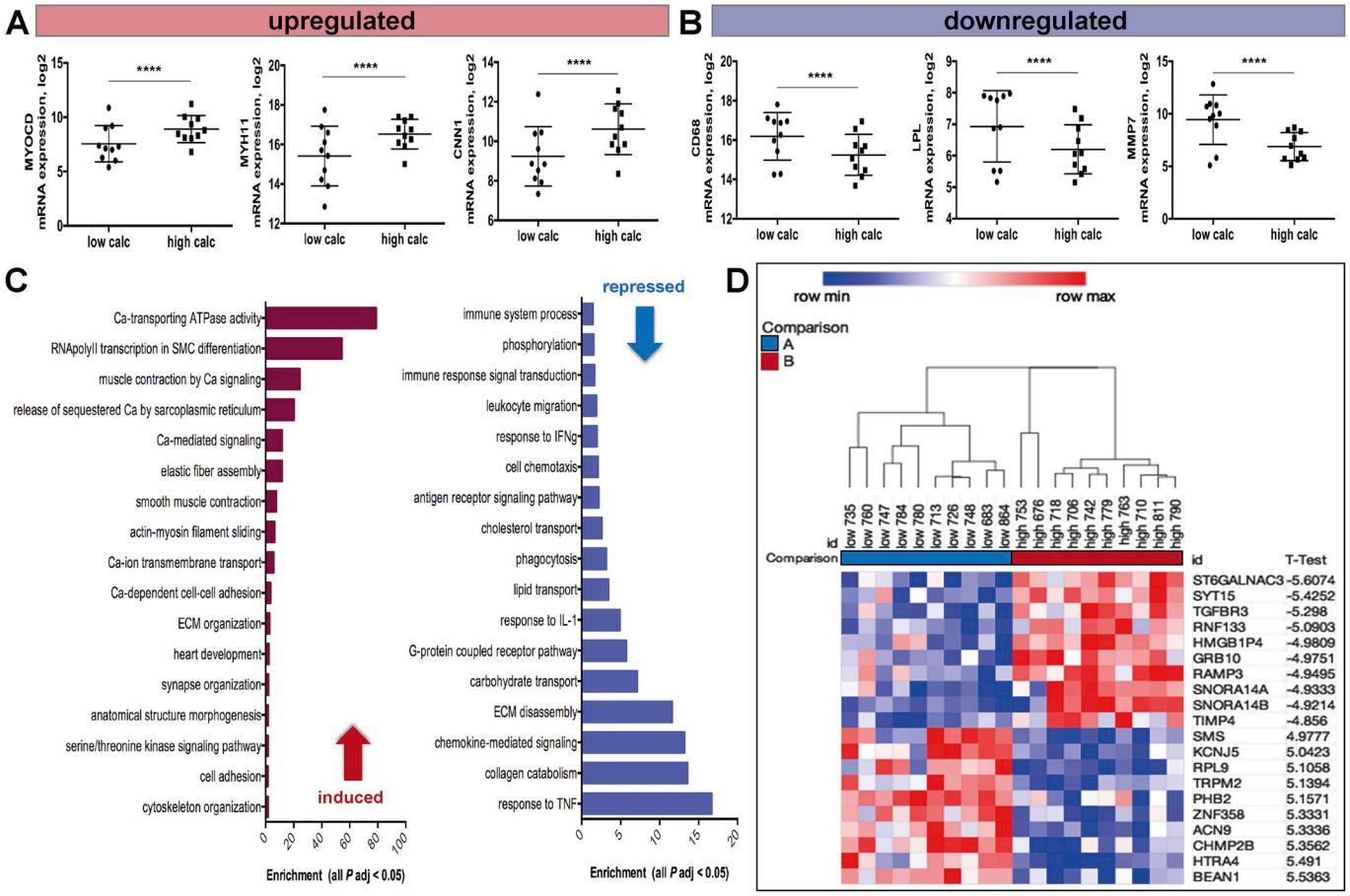

Fig. 2. SMC-related processes are induced in high-calcified plaques and inflammation is repressed.
(A) Microarray analysis comparing high *vs.* low calcified plaques showed upregulation of SMC contractility markers, and (B) downregulation of markers for macrophages (*CD68*), lipids (*LPL*) and ECM degradation (*MMP7*). Plots show mean log2 with SD. (C) Pathway analyses confirmed induction of processes related to calcification and SMC function in high-calcified plaques, and repression of inflammation, cholesterol metabolism response to cytokines. (D) Prediction modelling revealed a panel signature of 20 genes (y-axis) separating high *vs.* low calcified plaques with 100% accuracy. All genes were significant in comparison between high and low calcified plaques ($p < 0.01$). Clustering of patients into groups according to gene expression levels shown above the X-axis; red color refers to high and blue to low gene expression. $^{*}p < 0.05$, $^{**}p < 0.01$, $^{***}p < 0.001$, $^{****}p < 0.0001$. (For interpretation of the references to color in this figure legend, the reader is referred to the Web version of this article.)

differentially expressed genes, confirmed induction of processes related to Ca-signaling, but also to smooth muscle function (i.e. muscle contraction) in high calcified plaques (Fig. 2C, Supplementary Table VIII). In particular, calcification processes, markers of chondrocytes (*COL2A1, COL1A1, ACAN, MMP13*) and osteoblasts (*IGF1R, BMP4, SPARC, S100A4, SOST*) were upregulated in high-calcified plaques and strongly positively correlated to markers of contractile SMCs (*MYH11, ACTA2, LMOD1, SYNPO2*), while markers of osteoclasts were downregulated (*CSF1, OSCAR*) (Supplementary Tables IX and X). Overall, repression of processes associated with inflammation, ECM degradation, cholesterol metabolism, and response to cytokines was confirmed in high-calcified plaques (Fig. 2C, Supplementary Table VIII). Among the most repressed pathways were e.g. response to TNF, IL1, IFNg, phagocytosis and chemokine-mediated signaling.

In addition, we also studied the enrichment of subcellular compartments in plaques by comparing the predicted localization of differentially expressed genes from high *vs.* low calcified plaques in this study with those previously published in plaques from asymptomatic *vs.* symptomatic patients (Supplementary Fig. II) [8]. Here we also found that cytoskeletal localization was strikingly enriched in high calcified plaques, while nuclear and mitochondrial gene expression on the other hand seemed to be repressed, especially in comparison to plaques from asymptomatic patients.

However, despite substantial gene expression differences, principal components analysis for classification of patients in high *vs.* low calcified groups based on the global transcriptomic profiles could explain about 24% of the variance between groups (Supplementary Fig. III). By prediction modelling, we revealed a combined signature panel of 20 genes which was capable of considerably improving this separation and explaining up to 65% of the variance between groups (Fig. 2D). This panel comprised: genes involved in vesicle transport (*SYT15, CHMP2B*); *TGFBR3* that inhibits TGFB1 signaling; bone resorption inhibitor (*RAMP3*); protease inhibitors (*TIMP4, HTRA4*); and ion channels (*KCNJ5, TRPM2*).

Together, these bioinformatic analyses indicated that macro-calcification is not only a prominent morphological feature, but also associated with a distinct molecular phenotype of late-stage plaques and correlated with induction of processes traditionally linked with plaque-stabilization, while classical atherogenic and destabilizing processes were repressed.

3.3. Stabilising processes are also induced in calcified plaques from symptomatic patients

Next, we examined the molecular signature of calcified plaques particularly in relation to patient symptoms (Fig. 3A). Global gene expression analysis comparing plaques from S *vs.* AS high-calcified patients, resulted in totally 1900 significantly differentially expressed

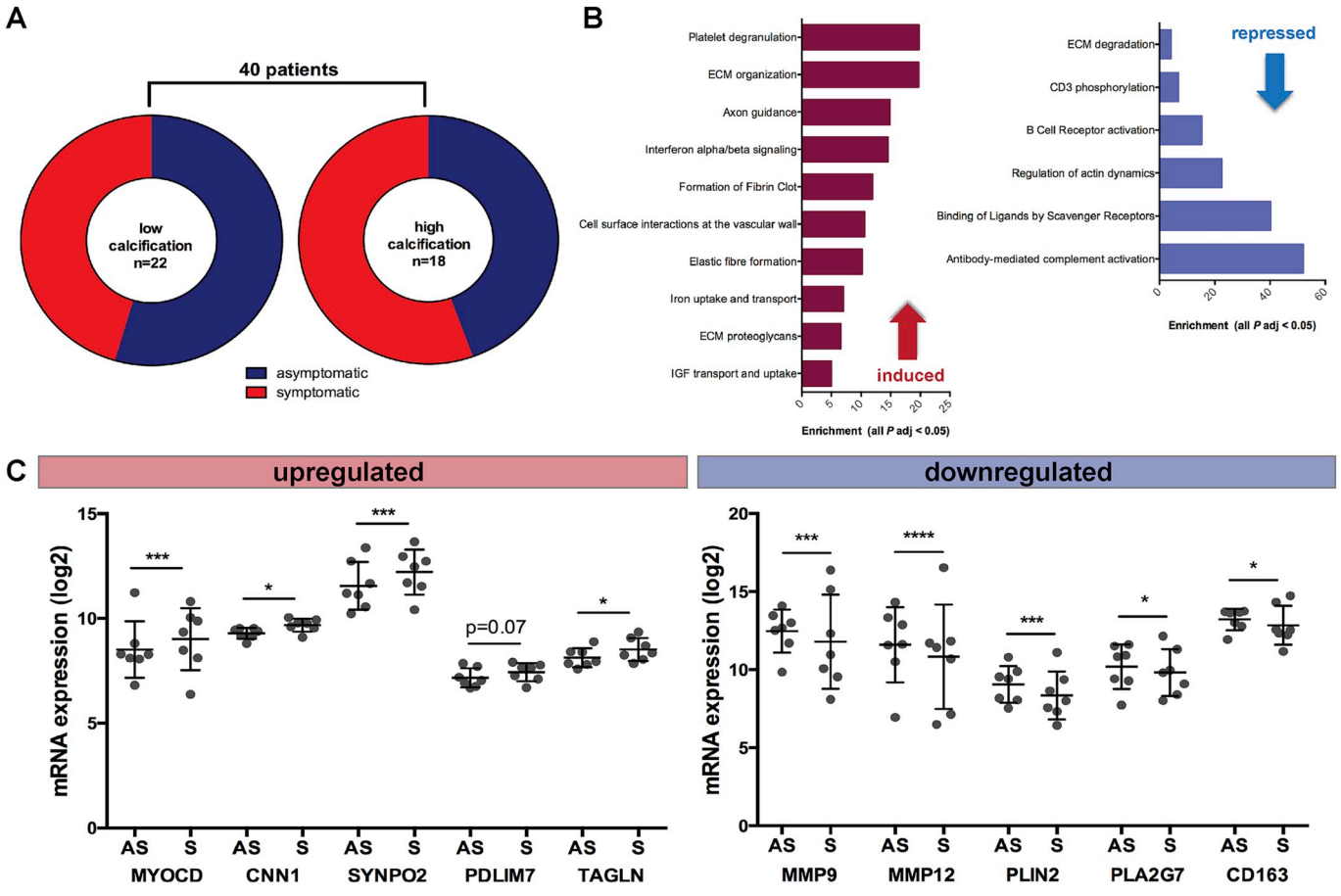

Fig. 3. Inflammation and tissue degradation are repressed in calcified plaques from symptomatic patients.
(A) From the whole cohort of 40 patients, association of calcification with patient symptomatology was assessed in a selected cohort of high-calcified plaques, where no significant differences were observed for other clinical parameters (n = 7 symptomatic *vs.* 7 asymptomatic patients). (B) Pathway analyses showed an expected induction of processes related to intra-plaque haemorrhage in high-calcified plaques from symptomatic patients, but also enrichment of extracellular matrix (ECM) and tissue organization. Inflammation and tissue-degradative processes were suppressed. (C) Microarray analysis showed an upregulation of SMC contractility markers, and downregulation of markers for macrophages, lipids and ECM degradation. Plots show mean log2 with SD. $*p < 0.05$, $**p < 0.01$, $***p < 0.001$, $****p < 0.0001$.

probesets (Bonferroni adjusted $p < 0.05$, Supplementary Tables XI and XII). In S patients, gene set enrichment and pathway analyses confirmed induction of processes related to intraplaque haemorhhage (i.e. fibrin clot formation, iron uptake and platelet degranulation), but also pointed to an enrichment of ECM organization *via* elastin and proteoglycans. Tissue degradation and immune-cell activation were repressed in high calcified plaques from S patients (Fig. 3B, Supplementary Table XIII). Here, we also noted an upregulation of both classical and novel SMC contractility markers [21], while markers of macrophages (*CD163*), lipid metabolism (*PLIN2, PLA2G7*) and ECM degradation (*MMP9, MMP12*) were downregulated (Fig. 3C, Supplementary Tables XI and XII). Additional gene expression data from this subset of patients for relevant markers is shown in Supplementary Fig. IB. This analysis revealed that macro-calcification consistently associates with features typical for plaque stabilization on molecular level, even in patients that have suffered symtoms.

Enhanced expression of SMC markers, elastin and collagen is common for intimal and medial calcification.

In order to investigate further the observed enrichment of SMC contractility and ECM genes in association to plaque calcification, we combined gene and tissue microarrays (TMA) for assessment of both mRNA and proteins (Fig. 4A). ACTA2 was found to be upregulated in high vs. low calcified plaques and strongly positively correlated with expression of ELN and collagen by gene microarrays. On protein level, TMAs confirmed strong positive association between plaque calcification and collagen content as well as between SMA and elastin/collagen content. Histological stainings revealed a repression of sensitive SMC markers (i.e. PDLIM7, LMOD1) in low calcified plaques [21], as well as ECM proteins (elastin, collagen, proteoglycans), but in high-calcified plaques all were abundant (Fig. 4B).

We next examined if the observed pattern of smooth muscle contractility and ECM genes also appeared in epigastric arteries with medial calcification from CKD patients (Supplementary Fig. IV). Quantitatively, by low-density qPCR arrays (LDA), a significant increase in *ACTA2* could be shown in association with calcification as well as a strongly positive correlation with expression of elastin and collagen (Supplementary Fig. IVA). In arteries with medial calcification we could also validate the positive correlation between *ACTA2* and calcification markers previously observed in high-calcified plaques (Pearson r [*ACTA2/BGLAP*] = 0.44, $p = 0.004$; Pearson r [*ACTA2/BMP2*] = 0.47, $p < 0.0001$). Histological staining demonstrated a similar expression pattern of SMC markers as observed in calcified plaques along with increased staining for elastin and collagen in the media (Supplementary Fig. IVB).

Active inflammation driven by $CD4^+$ cells, macrophages and mast cells is repressed in high calcified plaques.

The observed downregulation of inflammation markers and pathways in high calcified plaques was investigated further using the microarray deconvolution method, based on the expression of signature markers for 22 different leukocyte subtypes [22]. Our analyses confirmed that macrophages and $CD4^+$ cells are the most abundant immune cells in plaques generally (Fig. 5). Interestingly, low calcified plaques contained relatively more activated immune cells such as mast cells, NK cells, M0 macrophages and memory B cells, while high calcified plaques contained more resting $CD4^+$ and mast cells (Fig. 5A). Surprisingly, this pattern persists even when patients in this cohort are stratified according to symptoms, where the symptomatic but highly calcified ones appear to have less activated mast cells and M0 macrophages, and more protective M2 macrophages (Fig. 5B). Immunohistochemical analysis confirmed the basic differences in markers of active inflammation (i.e. macrophages CD68, activated mast cells Tryptase) between low and high calcified plaques (Fig. 5C).

Thus, using a combination of advanced bioinformatic and histological analyses, our data shows the induction of SMC- and ECM-related processes and dampened inflammation in high calcified lesions, even in those from symptomatic patients.

3.4. PRG4 is the top upregulated gene in high-calcified plaques

Numerous genes previously not associated with atherosclerosis were found to be highly upregulated in high *vs.* low calcified plaques (i.e. Nephronectin; Dermatopontin; Intelectin 1; Supplementary Table V). Proteoglycan 4 (*PRG4*) emerged as the most significantly upregulated gene in this comparison (9x fold change, adj $p < 0.0001$) (Supplementary Table V, Fig. 6A). This finding could be validated by microarrays in the whole cohort of 40 patients (Fig. 6B), and the same trend was confirmed by quantitative PCR in a small number of additional non-overlapping patients (Fig. 6C). In high calcified plaques from symptomatic vs. asymptomatic patients *PRG4* was still highly upregulated (5.8x fold change, adj $p < 0.0001$) (Fig. 6D, Supplementary Table XI), and was therefore selected for a more detailed investigation.

To delineate the functional associations of *PRG4*, expression of this gene was first correlated with the whole transcriptome in calcified plaques (Supplementary Fig. VA), which highlighted i.e. transcription factors *NFE2L2, MRPL* and *SMDT1* that mediate Ca uptake in mitochondria, Ca-binding *S100P* and the phagocytic receptor *VSIG4* (all Pearson r > 0.8) as the top correlated genes. Overall, *PRG4* associated with processes such as response to inorganic ion and chemokine signaling, but most enrichment was found for hematopoietic progenitor cell differentiation and inhibition of vascular SMC migration (Fig. 6E). Similarly, correlations of *PRG4* with markers of major cell types in calcified plaques were assessed (Supplementary Fig. VB), showing a weaker but positive association to both inflammatory and smooth muscle cells, and strongly positive with bone metabolism and osteolysis/osteoclasts (i.e. *IBSP, BMP2, SOX9, RUNX2, OSCAR,* TNFRSF11A*, ACP5/TRAP*), osteoarthritis markers (*TNFAIP6*), and also with some markers of inflammation inhibition (*CTLA4*).

On protein level, immunostaining (Fig. 6F, Supplementary Fig. VI) demonstrated that PRG4 was abundant in carotid plaques where it was localized mainly to the ECM in osteopontin (OPN) and osteocalcin (OCN) positive areas. In low calcified lesions, PRG4 was found in SMA + regions both intra- and extra-celullarly, while in high-calcified plaques it was observed in CD68+/TRAP + cells surrounding the macro-calcification nodules. However, abundant signal for PRG4 could not be observed in ECM of arteries with high medial calcification and instead only sporadic expression was noted (Supplementary Fig. VII).

4. Discussion

Here we investigated gene expression signatures and molecular pathways in high or low calcified carotid lesions as estimated by preoperative CTA. Our results demonstrated: i) that macro-calcification associates with processes typically related to a more stable plaque phenotype; ii) upregulated expression of SMC differentiation markers is concurrent with repression of inflammation and increased expression of calcification markers and ECM molecules in carotid plaques and in arteries with medial calcification; iii) *PRG4*, previously not described in atherosclerosis, is the most upregulated gene in high-calcified carotid plaques.

CTA estimation of carotid plaque calcification correlated to distinct gene expression profiles, even when patient symptomatology was taken into account. We cannot exclude that the latter findings at least partly could be explained by severe plaque heterogeneity (see limitations). Overall, biological processes related to SMC function and cell cytoskeleton were induced in high-calcified lesions, while processes typically associated with unstable lesions such as inflammation, ECM degradation, and cholesterol metabolism were repressed. By prediction modelling, a panel of 20 genes was enough to separate high from low calcified plaques with 100% accuracy. For comparison, we previously reported that a panel of 30 genes could discriminate plaques from S vs. AS patients with 78% accuracy [8]. Thus, our findings suggested that CTA can provide additional information on plaque phenotype, as opposed to comparisons based solely on patient phenotype, and support

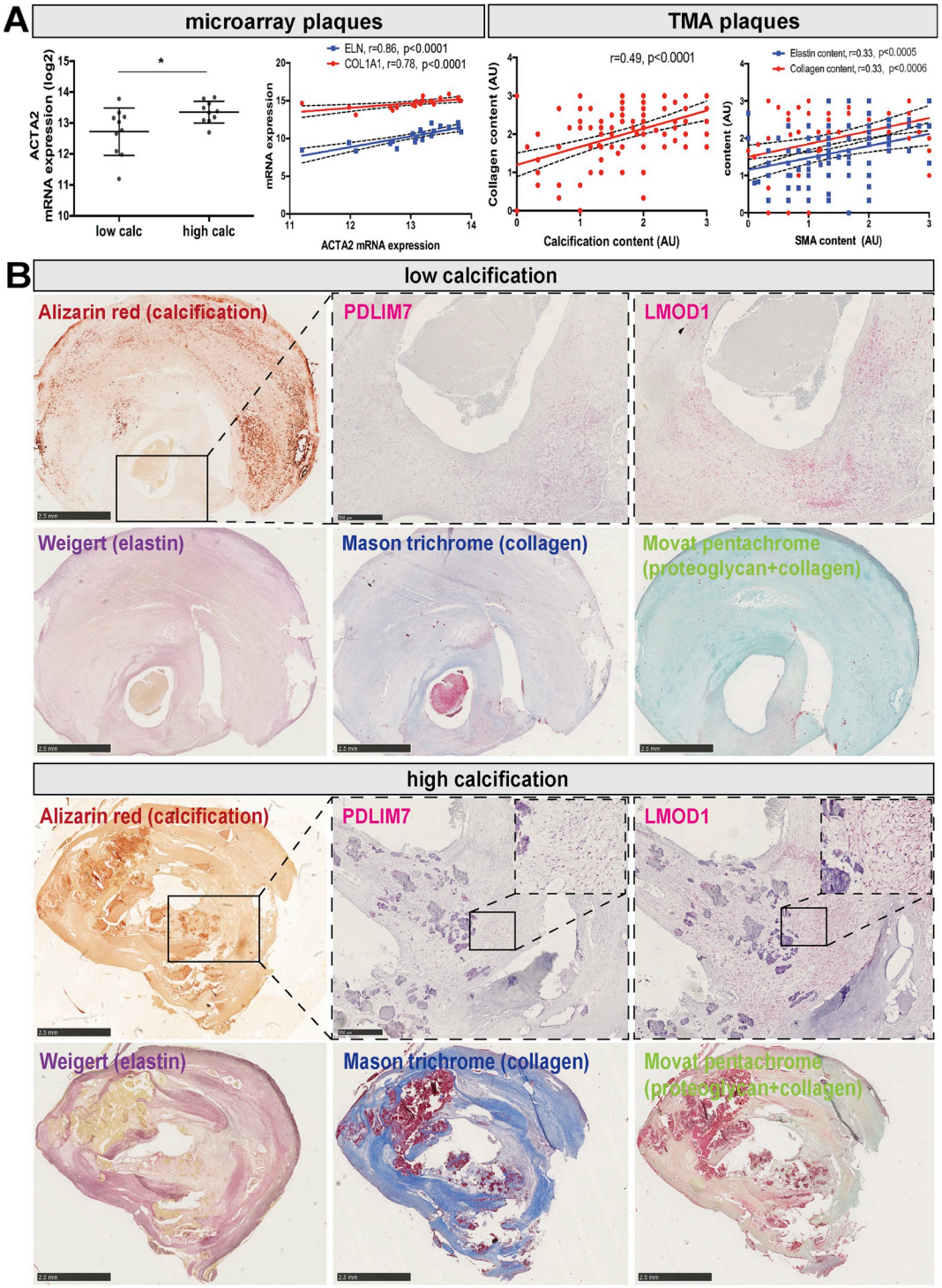

Fig. 4. Validation of SMC related changes in high-calcified plaques.
(A) By gene (left) and tissue (right) microarrays, increase in *ACTA2* was found in high-calcified plaques. *ACTA2* upregulation positively correlated with mRNA expression of elastin and collagen. Tissue microarrays (TMAs) validated the positive association between calcification and collagen content, and between SMA and elastin/collagen content (lower panels) on protein level. (B) Stainings showed abundant signal for SMC markers (*PDLIM7, LMOD1*), elastin (Weigert, dark purple), collagen (Masson trichrome, dark blue) and proteoglycans (Movat pentachrome, light green) in high-compared to low-calcified plaques (Alizarin Red). Images show 2× magnification, enlarged images show 40×. $*p < 0.05$, $**p < 0.01$, $***p < 0.001$, $****p < 0.0001$. (For interpretation of the references to color in this figure legend, the reader is referred to the Web version of this article.)

previous proposals that CTA estimation of calcification may aid prediction of stroke risk in patients with carotid disease [14].

This study was restricted to estimation of macro-calcification, which has previously been associated with more stable coronary lesions [24]. In contrast, micro-calcifications have been linked to unstable lesions in patients [25] and plaque inflammation in *ApoE*$^{-/-}$ mice [12]. Of the clinical parameters tested in our study, only creatinine and CRP positively correlated with calcification, whereas correlation with BMI was negative. The association between creatinine and calcification was expected as impaired renal function has an established role in progression

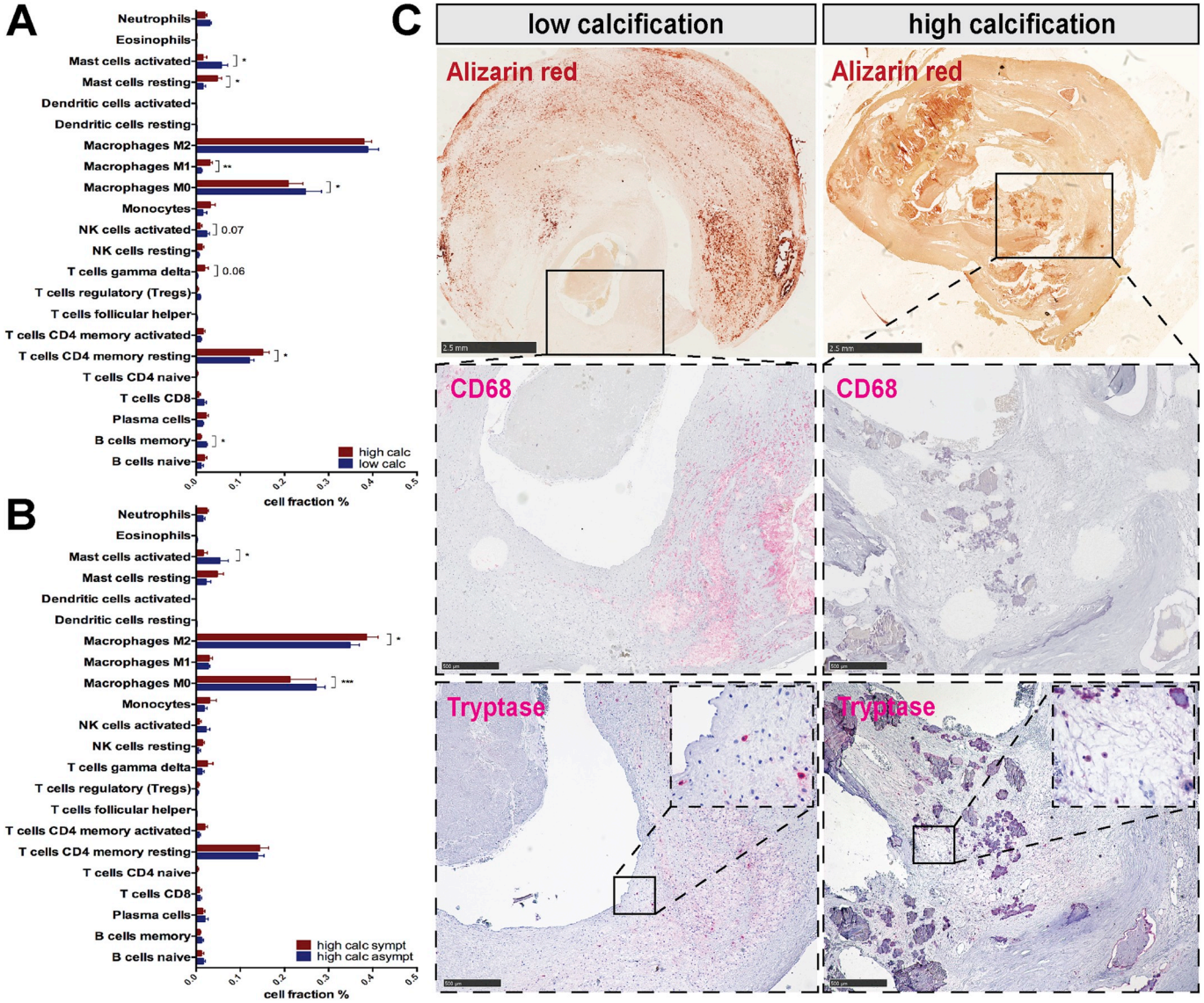

Fig. 5. Validation of inflammation related changes in calcified plaques.
(A) Deconvolution analysis based on microarrays from all n = 40 patients shows that low calcified plaques contain relatively more activated inflammatory cells (mast cells, NK cells, M0 macrophages and memory B cells), while high calcified plaques have a higher fraction of resting $CD4^+$ cells and mast cells. (B) A similar pattern persists in high calcified plaques stratified according to symptoms, where differences between lesions from asymptomatic and symptomatic patients are dominated by relative contributions of activated *vs.* resting mast cells and M0 *vs.* M2 macrophages. (C) Histological analysis illustrates the basic differences in markers of active inflammation (CD68, Tryptase) between low and high calcified plaques. Alizarin Red shows calcification. Images show 2x (Alizarin Red), 4x (CD68 and Tryptase), and enlarged images 40× magnification. $*p < 0.05$, $**p < 0.01$, $***p < 0.001$, $****p < 0.0001$. (For interpretation of the references to color in this figure legend, the reader is referred to the Web version of this article.)

of vascular calcification [26]. In support of our findings, BMI has previously been coupled to echolucent and low-calcified plaques by carotid ultrasound in diabetes patients [27]. While association between CRP and vascular calcification in CKD [28] has been shown, and CRP seems related to progression of carotid stenosis [29], a positive association to carotid calcification has not been shown before. Possibly, the moderate association found in our study reflects residual long-term systemic inflammation or increased vascular senescence in end-stage atherosclerosis, similarly as previously shown in CKD [9].

With respect to individual genes, expression of SMC markers was significantly elevated in high-calcified lesions, and strongly correlated to calcification genes. This finding shows that calcification in end-stage atherosclerosis can be present together with SMCs expressing contractility markers associated with a more differentiated phenotype. In atherogenesis, SMCs have been shown to undergo transition into cells of other lineages and calcification has been associated with transdifferentiation of SMCs into chondro- and osteoblast-like cells [30]. We and others have shown that SMC reacquire gene expression features typical for quiescent, differentiated phenotype during recovery after vascular injury [21] and our findings here imply that SMCs may also maintain or reestablish a differentiated SMC transcriptome in the presence of calcification, as opposed to a terminal transition into an osteo-chondrogenic phenotype. In support of these findings, calcifying SMCs *in vitro* were recently demonstrated to induce osteogenic pathways while maintaining the ability to express typical SMC contractile markers [7]. Moreover, by comparing high-calcified plaques and arteries with medial calcification, a process largely devoid of features associated with atherosclerosis [10], a similar sustained expression of SMC markers was observed. In both intimal and medial calcification, elastin and collagen levels, and in plaques also *HSPG2* (perlecan) levels, were strongly associated with expression of SMC contractility markers. We have previously shown that ECM can regulate the phenotypic state

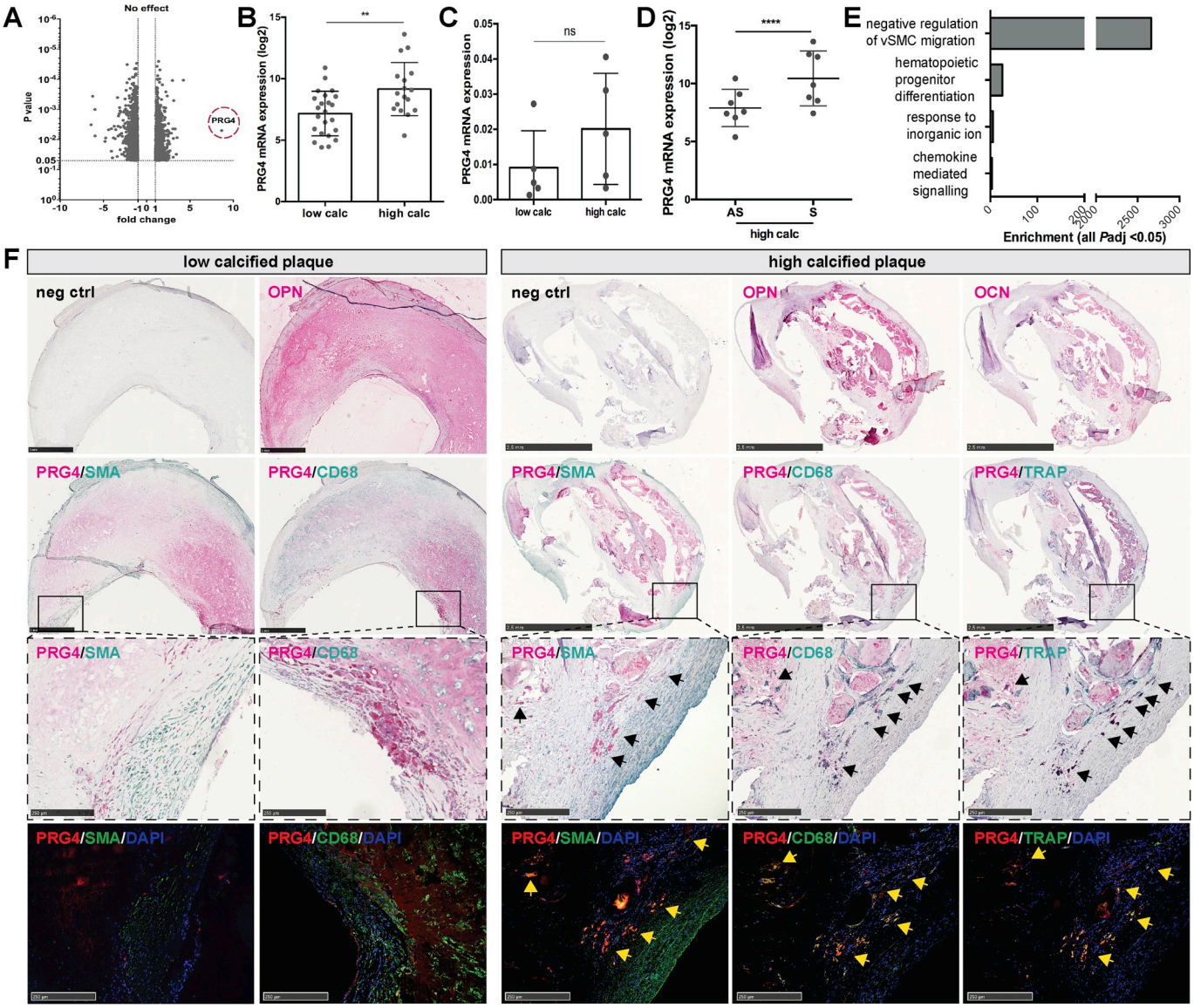

Fig. 6. PRG4 is upregulated in high-calcified plaques and localized to ECM and activated macrophages.
(A) Volcano plot showing that *PRG4* is the top significantly upregulated gene comparing all high (n = 18) *vs.* low (n = 22) calcified plaques. (B) Bar plot shows *PRG4* fold change and standard deviation among patients from microarrays. (C) By quantitative PCR from an additional non-overlapping set of patients, *PRG4* showed a non-significant trend towards upregulation in high-calcified plaques (n = 5 with high calcification degree 25–34% and n = 5 with low calcification 0–5%). (D) *PRG4* was also strongly upregulated comparing high calcified plaques from S (n = 7) *vs.* AS (n = 7) patients. (E) Top pathways associated with *PRG4* expression in calcified plaques microarrays. (F) Histological assessment by both immunohistochemistry and immunofluorescence confirms abundance of PRG4 in plaques, particularly in areas positive for an early marker of calcification, osteopontin (OPN) and osteocalcin (OCN). In low calcified plaques, PRG4 (red signal) is localized in the ECM surrounding the areas rich in both SMA+ and CD68 $^{+}$ cells (green signal) in the fibrous cap. In high-calcified plaques, PRG4 co-localizes with CD68+/TRAP + cells surrounding the macro-calcified nodules (enlarged areas). Images show 1.25x (low calcified), 2x (high calcified), and enlarged images 10× magnification. Nuclear staining with 4′,6-diamidino-2-phenylindole (DAPI). *$p < 0.05$, **$p < 0.01$, ***$p < 0.001$, ****$p < 0.0001$. For interpretation of the references to color in this figure legend, the reader is referred to the Web version of this article.)

of SMCs and that basement membrane components, such as perlecan, promote SMC quiescence and differentiation [31]. Although generally reduced in carotid atherosclerosis [32], the upregulation of *HSPG2* and the collagen- and elastin rich ECM observed in high-calcified plaques, suggests a pericellular environment that favors a more differentiated SMC phenotype [33,34]. Enrichment of these ECM components also indicated a more stable connective tissue, further supporting the association between plaque calcification and stability. Similarly, *in vitro* macro-calcification has been shown to increase cellular resistance to fluid sheer stress through enhanced cell-matrix interactions [35] and SMCs have a well-documented capacity to respond to physical forces and mechanical stretch [36]. Previous studies have already demonstrated elevated serum-titers of degraded elastin in patients with symptomatic carotid stenosis [37], increased stroke risk associated with low carotid plaque elastin content [38,39], and reduced elastin expression in plaques from S *vs.* AS patients [40].

Atherosclerosis is a chronic inflammatory disease where the contribution of various leukocyte subtypes has been extensively studied in the human context. Here, we were able to show that a dampening in active inflammation ongoing in the high-calcified lesions happens concurrently with increased stability via SMC- and ECM-related processes, even in lesions from symptomatic patients. These effects were mostly driven by differences in the relative fractions of active *vs.* resting mast cells, M0 *vs.* M2 macrophages and resting CD4^{+} cells. Interestingly and in agreement with our data, enrichment in mast cells and T-lymphocytes has recently been associated not only with a more

vulnerable plaque phenotype, but also with higher risk of adverse cardiovascular events in patients [41,42].

We also identified numerous ECM-related genes previously not associated with atherosclerosis, such as: Proteoglycan 4 (*PRG4*), Nephronectin, Dermatopontin, and Intelectin 1. Nephronectin and Dermatopontin are recently described ECM-related genes associated with osteoblast proliferation [43] and collagen fibrillogenesis [44], whereas Intelectin 1 is an adipokine [45]. Interestingly, *PRG4* was the most upregulated gene associated with intimal calcification in general and particularly in calcified plaques from S patients, but it was not prominently enriched in association with medial calcification. Expression of *PRG4* correlated with Ca-uptake and bone homeostasis genes, and with inhibition of SMC migration, while the protein was detected throughout the ECM and localized to SMA + and CD68 + /TRAP + cells surrounding calcification nodules. PRG4 is a mucinous glycoprotein secreted in joints by chondrocytes and synovial cells for boundary lubrication [46], recently linked with chondrogenic differentiation of mesenchymal stem cells [47]. Expression levels of *PRG4, SOX9* and *RUNX2* were positively correlated in plaques, suggesting that *PRG4* is connected to the formation of proteoglycan-rich collagenous matrix by chondrocyte-like cells, which may also be derived from transdifferentiated SMCs. Since the formation of vascular macro-calcifications has similarities with bone remodeling [48] and *PRG4* has not previously been associated with osteolysis, the staining of PRG4 in activated macrophages could represent protein remnants ingested after degradation and remodeling processes, but the specific function of *PRG4* in atherosclerotic plaque calcification remains to be determined.

With respect to limitations, the varying image acquisition protocols used at the different admitting hospitals did not include plain CT imaging before contrast enhancement, which may influence estimation of plaque calcification. In addition, the resolution of CTA imaging and the quantification software may not fully assess lesion morphology. However, in this specific cohort, CTA-resolution should not affect the measurements since the voxel size was $< 0.5\,mm^3$ and macro-calcifications are $> 1\,mm^3$. The advantage with this method is that these tools are in routine clinical use, which may facilitate clinical implementation. Similarly, the heterogeneous lesion composition may not be ideally represented by the sampling protocol used in the study that did not permit complete histological characterization of plaque phenotype. The lack of diagnostic tools for preoperative plaque phenotyping preclude accurate classification of lesion stability and we have in this study relied only on patient phenotyping with respect to clinical symptoms. We also acknowledge that validation of gene expression analyses obtained from microarrays was restricted as available material from human samples did not allow for complete independent validation. Nevertheless, the presented trends were supported by analysis of a bigger cohort and in case of PRG4, by qPCR analysis. In addition, the obtained correlations between calcification and biological processes were assessed in the proximal portion of the lesion while other features (i.e. of instability) may have been more prevalent in the distal part of the lesion that was not analysed by microarrays due to the study design. Since BiKE comprises only late-stage carotid plaques, processes related to disease progression could not be analysed and results are possibly not applicable to other vascular beds. Finally, the CKD cohort consisted of patients for living-donor transplantation, which constitute a selection of patients with less cardiovascular disease.

In summary, using a combination of clinical patient evaluation by CTA and plaque profiling with microarrays, we associate macro-calcification in advanced carotid lesions with molecular signatures typically linked to plaque stability, particularly related to alterations in SMC phenotype, ECM remodeling and repression of inflammation. Similar patterns were observed in CKD arteries with medial calcification, suggesting a commonality between these two etiologies. Our study generates a resource for further mechanistic investigations of plaque calcification addressing the role of specific molecular targets, such as *PRG4*. From a translational aspect, this study strengthens the notion that assessment of calcification by CTA can estimate plaque phenotype and stroke risk, and warrants larger, prospective cohort studies to evaluate the link between calcification and outcome in carotid patients.

Conflicts of interest

The authors declared they do not have anything to disclose regarding conflict of interest with respect to this manuscript.

Financial support

The European Union's Horizon 2020/Marie Sklodowska-Curie grant agreement No 722609 (INTRICARE); Swedish Heart and Lung Foundation; Swedish Research Council (K2009-65X-2233-01-3, K2013-65X-06816-30-4, 349-2007-8703); Uppdrag Besegra Stroke (P581/2011-123); Stockholm County Council (ALF2011-0260, ALF-2011-0279); Swedish Society for Medical Research; Tore Nilsson's, Magnus Bergvall's and Karolinska Institute Foundations.

Author contributions

EK, TS, ND, ML, MK, AW and LPM performed data analyses and experiments; HA and JRG provided technical support; JO, LM and PS provided material; LPM and UH designed and interpreted the study. All Authors participated in writing of the manuscript.

Acknowledgements

Surgeons from Karolinska University Hospital for the collection of patient material and Magnus Söderberg for calcification-grading of biopsies.

Appendix A. Supplementary data

Supplementary data to this article can be found online at https://doi.org/10.1016/j.atherosclerosis.2019.05.005.

References

[1] S. Chaturvedi, A. Bruno, T. Feasby, R. Holloway, O. Benavente, S.N. Cohen, R. Cote, D. Hess, J. Saver, J.D. Spence, B. Stern, J. Wilterdink, Therapeutics and technology assessment subcommittee of the American academy of N. Carotid endarterectomy–an evidence-based review: report of the therapeutics and technology assessment subcommittee of the American academy of neurology, Neurology 65 (2005) 794–801, https://doi.org/10.1212/01.wnl.0000176036.07558.82.

[2] A. Gupta, R.S. Marshall, Moving beyond luminal stenosis: imaging strategies for stroke prevention in asymptomatic carotid stenosis, Cerebrovasc. Dis. 39 (2015) 253–261, https://doi.org/10.1159/000381108.

[3] A.W. Aday, J.A. Beckman, Medical management of asymptomatic carotid artery stenosis, Prog. Cardiovasc. Dis. 59 (2017) 585–590, https://doi.org/10.1016/j.pcad.2017.05.008.

[4] A.V. Finn, M. Nakano, J. Narula, F.D. Kolodgie, R. Virmani, Concept of vulnerable/unstable plaque, Arterioscler. Thromb. Vasc. Biol. 30 (2010) 1282–1292, https://doi.org/10.1161/ATVBAHA.108.179739.

[5] D. Gomez, G.K. Owens, Smooth muscle cell phenotypic switching in atherosclerosis, Cardiovasc. Res. 95 (2012) 156–164, https://doi.org/10.1093/cvr/cvs115.

[6] A.N. Kapustin, C.M. Shanahan, Emerging roles for vascular smooth muscle cell exosomes in calcification and coagulation, J. Physiol. 594 (2016) 2905–2914, https://doi.org/10.1113/JP271340.

[7] R.D. Alves, M. Eijken, J. van de Peppel, J.P. van Leeuwen, Calcifying vascular smooth muscle cells and osteoblasts: independent cell types exhibiting extracellular matrix and biomineralization-related mimicries, BMC Genomics 15 (2014) 965, https://doi.org/10.1186/1471-2164-15-965.

[8] L. Perisic, S. Aldi, Y. Sun, L. Folkersen, A. Razuvaev, J. Roy, M. Lengquist, S. Akesson, C.E. Wheelock, L. Maegdefessel, A. Gabrielsen, J. Odeberg, G.K. Hansson, G. Paulsson-Berne, U. Hedin, Gene expression signatures, pathways and networks in carotid atherosclerosis, J. Intern. Med. 279 (2016) 293–308, https://doi.org/10.1111/joim.12448.

[9] P. Stenvinkel, K. Luttropp, D. McGuinness, A. Witasp, A.R. Qureshi, A. Wernerson, L. Nordfors, M. Schalling, J. Ripsweden, L. Wennberg, M. Soderberg, P. Barany, H. Olauson, P.G. Shiels, CDKN2A/p16INK4(a) expression is associated with vascular progeria in chronic kidney disease, Aging 9 (2017) 494–507, https://doi.org/10.18632/aging.101173.

[10] C.M. Shanahan, Mechanisms of vascular calcification in CKD-evidence for

premature ageing? Nat. Rev. Nephrol. 9 (2013) 661–670, https://doi.org/10.1038/nrneph.2013.176.
[11] K. Amann, Media calcification and intima calcification are distinct entities in chronic kidney disease, Clin. J. Am. Soc. Nephrol. 3 (2008) 1599–1605, https://doi.org/10.2215/CJN.02120508.
[12] E. Aikawa, M. Nahrendorf, J.L. Figueiredo, F.K. Swirski, T. Shtatland, R.H. Kohler, F.A. Jaffer, M. Aikawa, R. Weissleder, Osteogenesis associates with inflammation in early-stage atherosclerosis evaluated by molecular imaging in vivo, Circulation 116 (2007) 2841–2850, https://doi.org/10.1161/CIRCULATIONAHA.107.732867.
[13] T. Nakahara, M.R. Dweck, N. Narula, D. Pisapia, J. Narula, H.W. Strauss, Coronary artery calcification: from mechanism to molecular imaging, JACC Cardiovasc Imaging 10 (2017) 582–593, https://doi.org/10.1016/j.jcmg.2017.03.005.
[14] R.M. Kwee, Systematic review on the association between calcification in carotid plaques and clinical ischemic symptoms, J. Vasc. Surg. 51 (2010) 1015–1025, https://doi.org/10.1016/j.jvs.2009.08.072.
[15] W.E. Shaalan, H. Cheng, B. Gewertz, J.F. McKinsey, L.B. Schwartz, D. Katz, D. Cao, T. Desai, S. Glagov, H.S. Bassiouny, Degree of carotid plaque calcification in relation to symptomatic outcome and plaque inflammation, J. Vasc. Surg. 40 (2004) 262–269, https://doi.org/10.1016/j.jvs.2004.04.025.
[16] M. Sulkava, E. Raitoharju, A. Mennander, M. Levula, I. Seppala, L.P. Lyytikainen, O. Jarvinen, T. Illig, N. Klopp, N. Mononen, R. Laaksonen, M. Kahonen, N. Oksala, T. Lehtimaki, Differentially expressed genes and canonical pathways in the ascending thoracic aortic aneurysm - the Tampere Vascular Study, Sci. Rep. 7 (2017) 12127, https://doi.org/10.1038/s41598-017-12421-4.
[17] M. Steenman, O. Espitia, B. Maurel, B. Guyomarch, M.F. Heymann, M.A. Pistorius, B. Ory, D. Heymann, R. Houlgatte, Y. Goueffic, T. Quillard, Identification of genomic differences among peripheral arterial beds in atherosclerotic and healthy arteries, Sci. Rep. 8 (2018) 3940, https://doi.org/10.1038/s41598-018-22292-y.
[18] A.R. Naylor, P.M. Rothwell, P.R. Bell, Overview of the principal results and secondary analyses from the European and North American randomised trials of endarterectomy for symptomatic carotid stenosis, Eur. J. Vasc. Endovasc. Surg. 26 (2003) 115–129.
[19] A. Halliday, M. Harrison, E. Hayter, X. Kong, A. Mansfield, J. Marro, H. Pan, R. Peto, J. Potter, K. Rahimi, A. Rau, S. Robertson, J. Streifler, D. Thomas, G. Asymptomatic Carotid Surgery Trial Collaborative, 10-year stroke prevention after successful carotid endarterectomy for asymptomatic stenosis (ACST-1): a multicentre randomised trial, Lancet 376 (2010) 1074–1084, https://doi.org/10.1016/S0140-6736(10)61197-X.
[20] L. Perisic, E. Hedin, A. Razuvaev, M. Lengquist, C. Osterholm, L. Folkersen, P. Gillgren, G. Paulsson-Berne, F. Ponten, J. Odeberg, U. Hedin, Profiling of atherosclerotic lesions by gene and tissue microarrays reveals PCSK6 as a novel protease in unstable carotid atherosclerosis, Arterioscler. Thromb. Vasc. Biol. 33 (2013) 2432–2443, https://doi.org/10.1161/ATVBAHA.113.301743.
[21] L. Perisic Matic, U. Rykaczewska, A. Razuvaev, M. Sabater-Lleal, M. Lengquist, C.L. Miller, I. Ericsson, S. Rohl, M. Kronqvist, S. Aldi, J. Magne, V. Paloschi, M. Vesterlund, Y. Li, H. Jin, M.G. Diez, J. Roy, D. Baldassarre, F. Veglia, S.E. Humphries, U. de Faire, E. Tremoli, J. Odeberg, V. Vukojevic, J. Lehtio, L. Maegdefessel, E. Ehrenborg, G. Paulsson-Berne, G.K. Hansson, J.H. Lindeman, P. Eriksson, T. Quertermous, A. Hamsten, U. Hedin, Phenotypic modulation of smooth muscle cells in atherosclerosis is associated with downregulation of LMOD1, SYNPO2, PDLIM7, PLN, and SYNM, Arterioscler. Thromb. Vasc. Biol. 36 (2016) 1947–1961, https://doi.org/10.1161/ATVBAHA.116.307893.
[22] A.M. Newman, C.L. Liu, M.R. Green, A.J. Gentles, W. Feng, Y. Xu, C.D. Hoang, M. Diehn, A.A. Alizadeh, Robust enumeration of cell subsets from tissue expression profiles, Nat. Methods 12 (2015) 453–457, https://doi.org/10.1038/nmeth.3337.
[23] L.M. Orre, M. Vesterlund, Y. Pan, T. Arslan, Y. Zhu, A. Fernandez Woodbridge, O. Frings, E. Fredlund, J. Lehtio, SubCellBarCode: proteome-wide mapping of protein localization and relocalization, Mol. Cell 73 (2019) 166–182 e7, https://doi.org/10.1016/j.molcel.2018.11.035.
[24] P. Raggi, A. Boulay, S. Chasan-Taber, N. Amin, M. Dillon, S.K. Burke, G.M. Chertow, Cardiac calcification in adult hemodialysis patients. A link between end-stage renal disease and cardiovascular disease? J. Am. Coll. Cardiol. 39 (2002) 695–701.
[25] S. Motoyama, T. Kondo, M. Sarai, A. Sugiura, H. Harigaya, T. Sato, K. Inoue, M. Okumura, J. Ishii, H. Anno, R. Virmani, Y. Ozaki, H. Hishida, J. Narula, Multislice computed tomographic characteristics of coronary lesions in acute coronary syndromes, J. Am. Coll. Cardiol. 50 (2007) 319–326, https://doi.org/10.1016/j.jacc.2007.03.044.
[26] W.Y. Qunibi, Cardiovascular calcification in nondialyzed patients with chronic kidney disease, Semin. Dial. 20 (2007) 134–138, https://doi.org/10.1111/j.1525-139X.2007.00260.x.
[27] Y. Irie, N. Katakami, H. Kaneto, M. Takahara, K. Sakamoto, K. Kosugi, I. Shimomura, The risk factors associated with ultrasonic tissue characterization of carotid plaque in type 2 diabetic patients, J. Diabet. Complicat. 28 (2014) 523–527, https://doi.org/10.1016/j.jdiacomp.2014.03.009.
[28] K. Nitta, T. Akiba, K. Uchida, S. Otsubo, T. Takei, W. Yumura, T. Kabaya, H. Nihei, Serum osteoprotegerin levels and the extent of vascular calcification in haemodialysis patients, Nephrol. Dial. Transplant. 19 (2004) 1886–1889, https://doi.org/10.1093/ndt/gfh263.
[29] P.A. Stone, J. Kazil, The relationships between serum C-reactive protein level and risk and progression of coronary and carotid atherosclerosis, Semin. Vasc. Surg. 27 (2014) 138–142, https://doi.org/10.1053/j.semvascsurg.2015.04.002.
[30] V.P. Iyemere, D. Proudfoot, P.L. Weissberg, C.M. Shanahan, Vascular smooth muscle cell phenotypic plasticity and the regulation of vascular calcification, J. Intern. Med. 260 (2006) 192–210, https://doi.org/10.1111/j.1365-2796.2006.01692.x.
[31] P.K. Tran, K. Tran-Lundmark, R. Soininen, K. Tryggvason, J. Thyberg, U. Hedin, Increased intimal hyperplasia and smooth muscle cell proliferation in transgenic mice with heparan sulfate-deficient perlecan, Circ. Res. 94 (2004) 550–558, https://doi.org/10.1161/01.RES.0000117772.86853.34.
[32] P.K. Tran, H.E. Agardh, K. Tran-Lundmark, J. Ekstrand, J. Roy, B. Henderson, A. Gabrielsen, G.K. Hansson, J. Swedenborg, G. Paulsson-Berne, U. Hedin, Reduced perlecan expression and accumulation in human carotid atherosclerotic lesions, Atherosclerosis 190 (2007) 264–270, https://doi.org/10.1016/j.atherosclerosis.2006.03.010.
[33] U. Hedin, B.A. Bottger, E. Forsberg, S. Johansson, J. Thyberg, Diverse effects of fibronectin and laminin on phenotypic properties of cultured arterial smooth muscle cells, J. Cell Biol. 107 (1988) 307–319.
[34] U. Hedin, J. Roy, P.K. Tran, Control of smooth muscle cell proliferation in vascular disease, Curr. Opin. Lipidol. 15 (2004) 559–565.
[35] T.C. Lin, Y. Tintut, A. Lyman, W. Mack, L.L. Demer, T.K. Hsiai, Mechanical response of a calcified plaque model to fluid shear force, Ann. Biomed. Eng. 34 (2006) 1535–1541, https://doi.org/10.1007/s10439-006-9182-9.
[36] J.H. Haga, Y.S. Li, S. Chien, Molecular basis of the effects of mechanical stretch on vascular smooth muscle cells, J. Biomech. 40 (2007) 947–960, https://doi.org/10.1016/j.jbiomech.2006.04.011.
[37] P. Tzvetanov, V. Hegde, J.Y. Al-Hashel, M. Atanasova, A.P. Sohal, R.T. Rousseff, Abnormal levels of serum anti-elastin antibodies in patients with symptomatic carotid stenosis, Clin. Neurol. Neurosurg. 116 (2014) 9–12, https://doi.org/10.1016/j.clineuro.2013.11.011.
[38] G. Asciutto, N.V. Dias, A. Edsfeldt, M. Nitulescu, A. Persson, M. Nilsson, P. Duner, J. Nilsson, I. Goncalves, Low elastin content of carotid plaques is associated with increased risk of ipsilateral stroke, PLoS One 10 (2015) e0121086, , https://doi.org/10.1371/journal.pone.0121086.
[39] H. Mahdessian, L. Perisic Matic, M. Lengquist, K. Gertow, B. Sennblad, D. Baldassarre, F. Veglia, S.E. Humphries, R. Rauramaa, U. de Faire, A.J. Smit, P. Giral, S. Kurl, E. Mannarino, E. Tremoli, A. Hamsten, P. Eriksson, U. Hedin, A. Malarstig, Is group, Integrative studies implicate matrix metalloproteinase-12 as a culprit gene for large-artery atherosclerotic stroke, J. Intern. Med. 282 (2017) 429–444, https://doi.org/10.1111/joim.12655.
[40] A. Razuvaev, J. Ekstrand, L. Folkersen, H. Agardh, D. Markus, J. Swedenborg, G.K. Hansson, A. Gabrielsen, G. Paulsson-Berne, J. Roy, U. Hedin, Correlations between clinical variables and gene-expression profiles in carotid plaque instability, Eur. J. Vasc. Endovasc. Surg. 42 (2011) 722–730, https://doi.org/10.1016/j.ejvs.2011.05.023.
[41] S. Willems, A. Vink, I. Bot, P.H. Quax, G.J. de Borst, J.P. de Vries, S.M. van de Weg, F.L. Moll, J. Kuiper, P.T. Kovanen, D.P. de Kleijn, I.E. Hoefer, G. Pasterkamp, Mast cells in human carotid atherosclerotic plaques are associated with intraplaque microvessel density and the occurrence of future cardiovascular events, Eur. Heart J. 34 (2013) 3699–3706, https://doi.org/10.1093/eurheartj/eht186.
[42] H. Winkels, E. Ehinger, M. Vassallo, K. Buscher, H.Q. Dinh, K. Kobiyama, A.A.J. Hamers, C. Cochain, E. Vafadarnejad, A.E. Saliba, A. Zernecke, A.B. Pramod, A.K. Ghosh, N. Anto Michel, N. Hoppe, I. Hilgendorf, A. Zirlik, C.C. Hedrick, K. Ley, D. Wolf, Atlas of the immune cell repertoire in mouse atherosclerosis defined by single-cell RNA-sequencing and mass cytometry, Circ. Res. 122 (2018) 1675–1688, https://doi.org/10.1161/CIRCRESAHA.117.312513.
[43] M. Ikehata, A. Yamada, N. Morimura, M. Itose, T. Suzawa, T. Shirota, D. Chikazu, R. Kamijo, Wnt/beta-catenin signaling activates nephronectin expression in osteoblasts, Biochem. Biophys. Res. Commun. 484 (2017) 231–234, https://doi.org/10.1016/j.bbrc.2017.01.053.
[44] O. Okamoto, S. Fujiwara, Dermatopontin, a novel player in the biology of the extracellular matrix, Connect. Tissue Res. 47 (2006) 177–189, https://doi.org/10.1080/03008200600846564.
[45] K. Kawashima, K. Maeda, C. Saigo, Y. Kito, K. Yoshida, T. Takeuchi, Adiponectin and intelectin-1: important adipokine players in obesity-related colorectal carcinogenesis, Int. J. Mol. Sci. 18 (2017), https://doi.org/10.3390/ijms18040866.
[46] G.D. Jay, K.A. Waller, The biology of lubricin: near frictionless joint motion, Matrix Biol. 39 (2014) 17–24, https://doi.org/10.1016/j.matbio.2014.08.008.
[47] A.C.E. Graziano, R. Avola, G. Pannuzzo, V. Cardile, Aquaporin 1 and 3 modification as a result of chondrogenic differentiation of human mesenchymal stem cell, J. Cell. Physiol. (2017), https://doi.org/10.1002/jcp.26100.
[48] K.I. Bostrom, N.M. Rajamannan, D.A. Towler, The regulation of valvular and vascular sclerosis by osteogenic morphogens, Circ. Res. 109 (2011) 564–577, https://doi.org/10.1161/CIRCRESAHA.110.234278.